Decomposing stimulus-specific sensory neural information via diffusion models

Steeve Laquitaine*

Institut de la Vision, INSERM, CNRS Sorbonne Université 17 Rue Moreau, Paris 75012

Simone Azeglio*

Institut de la Vision, INSERM, CNRS, & Laboratoire des Systèmes Perceptifs Sorbonne University & École Normale Supérieure - PSL 17 Rue Moreau, Paris 75012 & 29 Rue d'Ulm Paris 75005

Carlo Paris

Institut de la Vision, INSERM, CNRS Sorbonne Université 17 Rue Moreau, Paris 75012

Ulisse Ferrari†

Institut de la Vision, INSERM, CNRS Sorbonne Université 17 Rue Moreau, Paris 75012

Matthew Chalk[†]

Institut de la Vision, INSERM, CNRS Sorbonne Université 17 Rue Moreau, Paris 75012 matthew.chalk@inserm.fr

Abstract

To understand sensory coding, we must ask not only how much information neurons encode, but also what that information is about. This requires decomposing mutual information into contributions from individual stimuli and stimulus features—a fundamentally ill-posed problem with infinitely many possible solutions. We address this by introducing three core axioms—additivity, positivity, and locality—that any meaningful stimulus-wise decomposition should satisfy. We then derive a decomposition that meets all three criteria and remains tractable for high-dimensional stimuli. Our decomposition can be efficiently estimated using diffusion models, allowing for scaling up to complex, structured and naturalistic stimuli. Applied to a model of visual neurons, our method quantifies how specific stimuli and features contribute to encoded information. Our approach provides a scalable, interpretable tool for probing representations in both biological and artificial neural systems.

1 Introduction

A central question in sensory neuroscience is *how much*, but also *what* information neurons transmit about the world. While Shannon's information theory provides a principled framework to quantify the amount of information neurons encode about *all* stimuli, it does not reveal *which* stimuli contribute most, or *what* stimulus features are encoded [Shannon, 1948, Brenner et al., 2000, DeWeese and

^{*}Equal contribution.

[†]Equal senior author contribution.

Meister, 1999]. As a concrete example, it is known that neurons in the early visual cortex are 'sensitive' to stimuli in a small region of space (their receptive field). However, it is not clear how such simple intuitions carry to more complex scenarios, e.g. with large, noisy & non-linear population of neurons and high-dimensional stimuli.

Several previous measures of neural sensitivity have been proposed. For example, the Fisher information quantifies the sensitivity of neural responses to infinitesimal stimulus perturbations [Rao, 1992, Brunel and Nadal, 1998, Yarrow et al., 2012, Kriegeskorte and Wei, 2021, Ding et al., 2023]. However, as the Fisher is not a valid decomposition of the mutual information it cannot say how different stimuli contribute to the total encoded information. On the other hand, previous works have proposed stimulus dependent decompositions of mutual information, which define a function I(x) such that $I(R;X) = \mathbb{E}[I(x)]$ [DeWeese and Meister, 1999, Butts, 2003, Butts and Goldman, 2006, Kostal and D'Onofrio, 2018]. However, this decomposition is inherently ill-posed: infinitely many functions I(x) satisfy the constraint, with no principled way to select among them. Further, different decompositions behave in qualitatively different ways, making it hard to interpret what are they are telling us. Finally, most proposed decompositions are computationally intractable for the high-dimensional stimuli and non-linear encoding models relevant for neuroscience.

To resolve these limitations, we propose a set of axioms that any stimulus specific and feature-specific information decomposition should satisfy in order to serve as a meaningful and interpretable measure of neural sensitivity. These axioms formalize intuitive desiderata: that the information assigned to each stimulus, and stimulus feature, should be non-negative, and additive with respect to repeated measurements. We also require the decomposition to respect a form of locality: changes in how a neuron responds to a stimulus x should not affect the information attributed to a distant stimulus x'. Finally, the attribution must be insensitive to irrelevant features, which do not contribute to the total information. Together, these constraints ensure that the decomposition is both interpretable and theoretically grounded.

We show that existing decompositions violate one or more of these axioms, limiting their interpretability and use as information theoretic measures of neural sensitivity. We then introduce a novel decomposition that satisfies all of our axioms. It generalizes Fisher information by capturing neural sensitivity to both infinitesimal and finite stimulus perturbations. Moreover, it supports further decomposition across individual stimulus features (e.g., image pixels), enabling fine-grained analysis of neural representations.

Beyond satisfying our theoretical axioms, our decomposition is computationally tractable for large neural populations and high-dimensional naturalistic stimuli, through the use of diffusion models. We demonstrate the power of our method by quantifying the information encoded by a model of visual neurons about individual images and pixels. Our approach uncovers aspects of the neural code that are not picked up by standard methods, such as the Fisher information, and opens the door to similar analyses in higher-order sensory areas, and artificial neural networks.

2 Desired properties of stimulus-specific decomposition of information

We aim to decompose the mutual information I(R; X) between a stimulus X and a neural response R into local attributions I(x), assigning to each stimulus x a measure of its contribution to the total information. By construction, such a decomposition must satisfy:

• Axiom 1: Completeness. The average of local attributions must recover the total mutual information:

$$I(R;X) = \mathbb{E}_X[I(x)]. \tag{1}$$

This constraint alone does not uniquely determine the function I(x), as many decompositions satisfy completeness. To further constrain the attribution, we impose additional desiderate that reflect desirable properties of local information measures.

First, for I(x) to serve as an *interpretable*, stimulus-specific measure of neural sensitivity, it should satisfy a *locality principle*: perturbations to the likelihood &/or prior in a neighbourhood of x_0 should have a vanishing influence on I(x) for distant stimuli $x \neq x_0$. Without this property, changes in I(x) may reflect changes in neural sensitivity to any stimuli, undermining interpretability.

• Axiom 2: Locality. Let p(R, X) and $\tilde{p}(R, X)$ be two joint distributions over the response, R, and stimulus, X. Suppose there exists finite $\epsilon > 0$ and x_0 such that:

$$p(R,x) = \tilde{p}(R,x)$$
 for all $x \notin B_{\epsilon}(x_0)$, (2)

where $B_{\epsilon}(x_0)$ is the open ball of radius ϵ centered at x_0 . Assuming X has infinite support on an unbounded or semi-infinite domain, we require that, for every $\delta > 0$ there should exist some finite value d, such that:

$$|I(x) - \tilde{I}(x)| \le \delta$$
 for all $x \notin B_d(x_0)$, (3)

where I(x) and $\tilde{I}(x)$ denote the corresponding information decompositions derived from p(R,x) and $\tilde{p}(R,X)$, respectively. That is, local perturbations to the likelihood or prior near x_0 should not affect the information assigned to distant stimuli, x.

Mutual information is globally non-negative: $I(R;X) \ge 0$. To preserve this property in our decomposition, we require the pointwise contributions I(x) to be non-negative as well. Intuitively, observing a neural response can only refine our beliefs about the stimulus—it cannot undo information. In addition, negative attributions can harm interpretability, since they can cancel out, obscuring how different stimuli contribute to the total information.

• Axiom 3: Positivity. Local information attributions must be non-negative:

$$I(x) \ge 0 \quad \text{for all} \quad x \in X.$$
 (4)

Finally, Shannon 1948 posited additivity as a fundamental property of mutual information: the total information from multiple sources should equal the sum of their individual contributions. We extend this principle pointwise, requiring that information combine additively across measurements.

Axiom 4: Additivity. For two responses R and R', the local attribution should decompose
as:

$$I_{R,R'}(x) = I_R(x) + I_{R'|R}(x), \quad \text{for all} \quad x \in X$$
 (5)

where we have renamed I(x) as $I_R(x)$ here, to make explicit its dependence on the response, R. $I_{R'|R}(x)$ is the conditional pointwise information from R' given R, and $I_{R,R'}(x)$ denotes the pointwise information from observing both responses. By construction, we require: $I(R';X|R) = E_x \left[I_{R'|R}(x)\right]$ and $I(R,R';X) = E_x \left[I_{R,R'}(x)\right]$.

Remark 1: Local data processing inequality. Any decomposition that fulfils both additivity and positivity, as stated above, also obeys a local form of the data processing inequality. That is, post-processing should not increase information, even at the level of the individual attributions. Formally,

If
$$X \to R \to R'$$
, then $I_R(x) \ge I_{R'}(x)$ for all $x \in X$ (6)

To prove this we use additivity to write $I_{R',R}(x)$ in two ways:

$$I_R(x) + I_{R'|R}(x) = I_{R'}(x) + I_{R|R'}(x)$$
(7)

Positivity gives $I_{R|R'}(x) \ge 0$ for all x, so:

$$I_R(x) + I_{R'|R}(x) \ge I_{R'}(x)$$
 (8)

Now, if R' is independent of X given R, then $I(R';X|R) = \mathbb{E}_X[I_{R'|R}(x)] = 0$. Since if $I_{R'|R}(x) \ge 0$ pointwise, this implies $I_{R'|R}(x) = 0$ for all x. Substituting into the inequality above yields the desired result: $I_R(x) \ge I_{R'}(x)$.

Remark 2: Invariance to invertible transformations. The data processing inequality implies that local information attributions are invariant under invertible transformations of the response variable. That is, for any invertible function $\phi(R)$, we have:

$$I_{\phi(R)}(x) = I_R(x). \tag{9}$$

This follows from the fact that $I(R;X) = I(\phi(R);X)$, and hence $\mathbb{E}_X[I_{\phi(R)}(x)] = \mathbb{E}_X[I_R(x)]$. Supposing, for contradiction, that $I_{\phi(R)}(x) < I_R(x)$ for some x, equality of expectations would require $I_{\phi(R)}(x) > I_R(x)$ for some other x, violating the pointwise data processing inequality. This highlights why our axioms are important for interpretability: they imply that I(x) quantifies how information is transmitted through the system $X \to R$, independently of how the responses are parameterized.

Table 1: Satisfaction of axioms by different information-theoretic measures of neural sensitivity. Only our proposed decomposition, I_{local} , fulfils all the axioms.

Axiom	$\mathcal{J}(x)$	$I_{sp}(x)$	$I_{SSI}(x)$	$I_{surp}(x)$	$I_{CiSSI}(x)$	$I_{local}(x)$
Completeness	Х	\checkmark	√	√	✓	\checkmark
Locality	\checkmark	X	×	×	×	\checkmark
Positivity	\checkmark	X	×	\checkmark	\checkmark	\checkmark
Additivity	\checkmark	\checkmark	\checkmark	\checkmark	\checkmark	\checkmark

3 Previous stimulus-dependent decompositions

Several previous works have proposed decompositions of mutual information into stimulus-specific contributions, such as the stimulus-specific information I_{SSI} [Butts, 2003], the specific information I_{sp} , the stimulus-specific surprise I_{surp} , [DeWeese and Meister, 1999], and the coordinate-invariant stimulus-specific information I_{CiSSI} [Kostal and D'Onofrio, 2018]:

$$I_{sp}(x) = H(R) - H(R|x) \tag{10}$$

$$I_{SSI}(x) = H(X) - \mathbb{E}_{R|x} \left[H(X|R=r) \right]$$
(11)

$$I_{surp}(x) = D_{KL} \left(p(R|x) || p(R) \right) \tag{12}$$

$$I_{CiSSI}(x) = \mathbb{E}_{R|x} \left[D_{KL} \left(p(X|R=r) || p(X) \right) \right]. \tag{13}$$

While these decompositions satisfy some of our proposed axioms (Table 1), none satisfy locality. This is because they all depend on global terms such as the marginal response distribution $p(r) = \int p(r|x')p(x')\,dx'$, or the posterior $p(x|r) = p(r|x)p(x)/\int p(r|x')p(x')\,dx'$, both of which can be influenced by changes to the likelihood &/or prior for any stimulus. Further, the requirement that $I_{CiSSI}(x)$ is invariant to invertible transformations of x is incompatible with locality; both axioms can't be fulfilled simultaneously. As discussed above, this limits the interpretability of previous decompositions as measures of neural sensitivity, since a non-zero attribution at x could be due to changes in neural sensitivity anywhere in the stimulus space.

Unlike the above decompositions, the Fisher information is inherently local. However, while previous authors found a relation between the Fisher and mutual information [Brunel and Nadal, 1998, Wei and Stocker, 2016], this only holds approximately, and in certain limits (e.g. low-noise). Therefore, the Fisher information cannot be used to quantify how different stimuli contribute to the total encoded information (i.e. it fails the **completeness** axiom).

Recently Kong et al. 2024 used diffusion models to decompose the mutual information into contributions from both the stimulus, x, and the response, r. Two different decompositions, I(r,x), were proposed. However, averaging these over p(R|x) does not give stimulus-wise decompositions that fulfil our axioms (Appendix B). In one case, we obtain $I_{surp}(x)$ (Eqn 12), which is non-local; in the other case, the decomposition is not additive, which is a fundamental information theoretic constraint.

In the following we propose a new stimulus-wise decomposition of the mutual information which fulfils all our axioms, combining the advantages of the Fisher information (locality, positivity & additivity) while being a valid decomposition of the mutual information.

4 Diffusion-based information decomposition

We first derive an expression for the mutual information, I(R; X), that can be used to construct a stimulus-dependent decomposition that fulfils all of the above axioms.

4.1 Exact relation between Shannon information and Fisher information

We consider a population of neurons which show a response, R, to a stimulus, X, with probability p(R|X). We then consider a noise-corrupted version of the stimulus, $X_{\gamma} = X + \sqrt{\gamma}Z$, where $Z \sim \mathcal{N}(0, I)$. From the fundamental theorem of calculus we can write:

$$-\int_{\gamma_0}^{\infty} \frac{dI(X_{\gamma}; R)}{d\gamma} d\gamma = I(R; X_{\gamma_0}) - \lim_{\gamma \to \infty} I(R; X_{\gamma}) = I(R; X_{\gamma_0}), \tag{14}$$

since in the limit $\gamma \to \infty$, X_{γ} is just noise, and thus $I(R; X_{\gamma}) \to 0$. It follows that,

$$I(R; X_{\gamma_0}) = -\int_{\gamma_0}^{\infty} \frac{dI(X_{\gamma}; R)}{d\gamma} d\gamma = \int_{\gamma_0}^{\infty} \left(\mathbb{E}_{p(R)} \left[\frac{dh(X_{\gamma}|r)}{d\gamma} \right] - \frac{dh(X_{\gamma})}{d\gamma} \right) d\gamma \tag{15}$$

where $h\left(X_{\gamma}\right) \equiv -\mathbb{E}_{p(X_{\gamma})}\left[\log p(X_{\gamma})\right]$ and $h\left(X_{\gamma}|r\right) \equiv -\mathbb{E}_{p(X_{\gamma}|r)}\left[\log p\left(X_{\gamma}|r\right)\right]$. Assuming that p(X) and p(X|R) have finite second order moments, we can apply de Bruijn's identity for all $\gamma > 0$, to obtain,

$$I(R; X_{\gamma_0}) = -\frac{1}{2} \operatorname{Trace} \int_{\gamma_0}^{\infty} \mathbb{E}_{p(X_{\gamma}, R)} \left[\nabla_{x_{\gamma}}^2 \log p \left(X_{\gamma} | R \right) - \nabla_{x_{\gamma}}^2 \log p \left(X_{\gamma} \right) \right] d\gamma$$

$$= -\frac{1}{2} \operatorname{Trace} \int_{\gamma_0}^{\infty} \mathbb{E}_{p(X_{\gamma}, R)} \left[\nabla_{x_{\gamma}}^2 \log p \left(R | X_{\gamma} \right) \right] d\gamma$$

$$= \frac{1}{2} \operatorname{Trace} \int_{\gamma_0}^{\infty} \mathbb{E}_{p(X_{\gamma})} \left[\mathcal{J} \left(X_{\gamma} \right) \right] d\gamma$$
(16)

where $\mathcal{J}(x_{\gamma})$ is the Fisher information with respect to a noise-corrupted stimulus, X_{γ} . Finally, since $\lim_{\gamma_0 \to 0} I(R; X_{\gamma_0}) = I(R; X)$, and $\operatorname{Trace}(E_{p(X_{\gamma})}[J(X_{\gamma})])$ is always non-negative, monotone convergence yields:

$$I(R;X) = \frac{1}{2} \operatorname{Trace} \int_{0}^{\infty} \mathbb{E}_{p(X_{\gamma})} \left[\mathcal{J} \left(X_{\gamma} \right) \right] d\gamma. \tag{17}$$

This is a general result that holds for both discrete and continuous X and R, so long as p(X) and p(X|R) have finite first and second moments.

The above identity provides a direct relation between the mutual information I(R;X) and the Fisher information, $\mathcal{J}(x_\gamma)$. Further, it also admits a natural interpretation in terms of de-noising diffusion models trained to predict X from a noisy observation X_γ . To see this, first we use an alternative formulation of the Fisher information, in terms of the mean-squared score:

$$I(R;X) = \frac{1}{2} \int_{0}^{\infty} \mathbb{E}_{p(X_{\gamma},R)} \left[\left\| \nabla_{x_{\gamma}} \log p\left(R|X_{\gamma}\right) \right\|^{2} \right] d\gamma$$

$$= \frac{1}{2} \int_{0}^{\infty} \mathbb{E}_{p(X_{\gamma},R)} \left[\left\| \nabla_{x_{\gamma}} \log p\left(X_{\gamma}|R\right) - \nabla_{x_{\gamma}} \log p\left(X_{\gamma}\right) \right\|^{2} \right] d\gamma \qquad (18)$$

Next, from Tweedie's formula [Meng et al., 2021, Kadkhodaie and Simoncelli, 2020] we have:

$$I(R;X) = \int_0^\infty \frac{1}{2\gamma^2} \mathbb{E}_{p(X_\gamma,R)} \left[\left\| \hat{x}(X_\gamma,R) - \hat{x}(X_\gamma) \right\|^2 \right] d\gamma, \tag{19}$$

where $\hat{x}(x_{\gamma}) = \mathbb{E}[X|x_{\gamma}]$ and $\hat{x}(x_{\gamma}, r) = \mathbb{E}[X|x_{\gamma}, r]$. These conditional means can be approximated using denoising diffusion models trained to sample from the prior, p(X), and posterior $p(X \mid R)$, respectively [Sundararajan et al., 2017].

4.2 Local stimulus-specific information

Building on the integral representation of mutual information in Eqn 17, we define a stimulus-specific decomposition:

$$I_{local}(x) = \frac{1}{2} \sum_{i} \int_{0}^{\infty} \mathbb{E}_{p(X_{\gamma}|x)} \left[\mathcal{J}_{ii}(X_{\gamma}) \right] d\gamma, \tag{20}$$

where $X_{\gamma} = x + \sqrt{\gamma}Z$, with $Z \sim \mathcal{N}(0, I)$, and $\mathcal{J}_{ii}(x_{\gamma}) = \mathbb{E}_{p(R|x_{\gamma})} \left[-\nabla^2_{(x_{\gamma})_i} \log p(R \mid x_{\gamma}) \right]$ is the i^{th} diagonal element of the Fisher information matrix, evaluated at x_{γ} . This expression parallels Eq. 17, with the key distinction that the expectation is now conditioned on a fixed stimulus x, rather than averaging over the full stimulus distribution x_{γ} . Consequently, the decomposition satisfies the **completeness axiom**, since by construction, $I(R;X) = \mathbb{E}\left[I_{local}(x)\right]$.

³Note that the exchange of integrals over γ and x_{γ} to go from Eqn 17 to Eqn 20 is justified by the fact that the integrand, $\mathcal{J}_{ii}(x_{\gamma})$, is Lebesgue integrable, since it is always positive and integrates to a finite value.

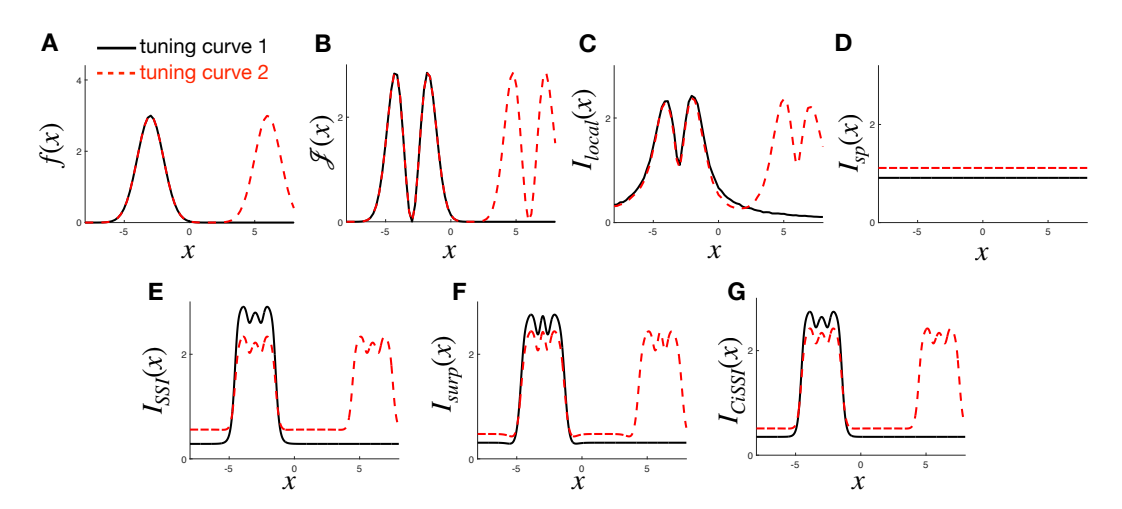


Figure 1: **Demonstration of locality.** (A) A neuron responds to a 1D stimulus x with tuning curve f(x). We compare two cases: (i) tuning changes only near x=-3 (black), and (ii) additional changes near x=6 (red dashed). (B–C) The Fisher information, $\mathcal{J}(x)$ and local information $I_{\text{local}}(x)$ converge as we go far from the region where the two tuning curves differ. (C–F) For other decompositions (Eqs. 10–13), local changes in the tuning curve result in non-local changes to the information attribution, for all x.

Next we outline why our decomposition fulfils the **locality axiom** (for the formal proof, see Appendix A). Recall that the Fisher information matrix $\mathcal{J}(x)$ characterizes the local curvature of the log-likelihood, $\log p(R\mid x)$, and thus quantifies the local sensitivity of the response to changes in the stimulus [Rao, 1992]. The term $\mathbb{E}_{X_\gamma\mid x}\left[\mathcal{J}(X_\gamma)\right]$ generalizes this notion, measuring neural sensitivity when we only observe noise-perturbed versions of the stimulus, $X_\gamma\sim\mathcal{N}(x,\gamma I)$. For finite γ , this term is dominated by values of X_γ close to x, and thus, it depends only on the local shape of the likelihood and prior around x. It receives a vanishingly small contribution from changes to the likelihood and/or prior for distant stimuli x', if $\|x'-x\|\gg\sqrt{\gamma}$. Meanwhile, as $\gamma\to\infty$, X_γ becomes pure noise and thus $E_{p(X_\gamma\mid x)}\left[\mathcal{J}(X_\gamma)\right]\to 0$ for all x. Taken together, this implies that our decomposition, obtained by integrating $E_{p(X_\gamma\mid x)}\left[\mathcal{J}(X_\gamma)\right]$ over all $\gamma>0$, satisfies the **locality axiom**: local perturbations to p(R,x) affect $I_{local}(x')$ only for nearby x', while their influence vanishes as $\|x'-x\|\to\infty$.

The remaining axioms follow directly from standard properties of the Fisher information matrix. **Positivity** follows from the fact that the Fisher information is positive semi-definite. **Additivity** follows from the identity $\mathcal{J}_{R',R}(x_\gamma) = \mathcal{J}_R(x_\gamma) + \mathcal{J}_{R'|R}(x_\gamma)$ [Zamir, 1998]. Both properties are preserved when we average the Fisher information over $p(X_\gamma|x)$ and integrate over $\gamma > 0$, to obtain $I_{local}(x)$.

4.3 Feature-Wise Decomposition

We assume the stimulus x is a vector of image features x_i (e.g. image pixels). Given that the local stimulus information (Eqn. 20) is expressed as a sum over diagonal elements of the Fisher information matrix, it is natural to decompose $I_{local}(x)$ into feature-wise contributions $I_i(x)$.

As with the stimulus-wise decomposition, this problem is ill-posed: infinitely many decompositions exist in theory. However, the same axioms constrain the feature-wise decomposition. To satisfy **additivity**, $I_i(x)$ must be a linear combination of Fisher diagonal terms: $I_i(x) = \frac{1}{2} \sum_j a_{ij} \int_0^\infty \mathbb{E}_{X_\gamma|x} [\mathcal{J}_{jj}(X_\gamma)] \, d\gamma$. **Completeness** requires $\sum_i a_{ij} = 1$, while **positivity** enforces $a_{ij} \geq 0$. Finally, to fully specify the weights, a_{ij} , we need to introduce one further axiom, which ensures that the attribution $I_i(x)$ is zero for irrelevant stimulus features, X_i , which are independent of the response, R.

Axiom 5: Insensitivity to irrelevant features. If X_i is independent of R, then I_i(x) = 0
 ∀x ∈ X.

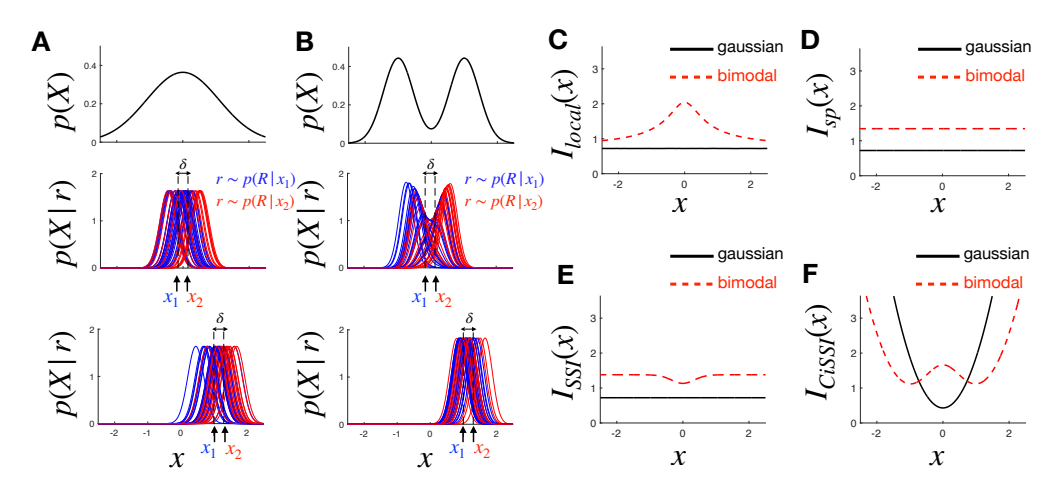


Figure 2: **Effect of prior.** (**A**) A gaussian prior (top) with a neuron responding as r=x+ noise. Middle and bottom: posterior $p(X\mid r)$ given $r\sim p(R\mid x_1)$ (blue) or $r\sim p(R\mid x_2)$ (red), for stimuli x_1,x_2 separated by δ . The posterior is equally sensitive to x near 0 (middle) than near 1 (bottom). (**B**) Same as A, but with bimodal prior (top). The posterior is more sensitive to x near 0 (middle) than near 1 (bottom). (**C**) The local information peaks near x=0 for the bimodal prior (red dashed), where the posterior is most sensitive, and is flat for a Gaussian prior (black), where posterior shape is constant. (**D-F**) Other decompositions behave differently: (D) $I_{\rm sp}$ is flat for both priors; (E) $I_{\rm SSI}$ is minimal near x=0 for the bimodal prior; (F) $I_{\rm CiSSI}$ is quadratic under a Gaussian prior. I_{surp} (not shown) behaves similarly to $I_{\rm CiSSI}$.

For this axiom to hold, we need to set $a_{ij} = \delta_{ij}$, so that $I_i(x) = \frac{1}{2} \int_0^\infty \mathbb{E}_{X_\gamma|x}[\mathcal{J}_{ii}(X_\gamma)] \, d\gamma$. If, on the contrary, $a_{ij} \neq \delta_{ij}$, then a neuron's sensitivity to other features (i.e. $\mathcal{J}_{jj}(x) > 0$) could 'leak over' to make $I_i(x) > 0$ even when X_i is independent of R, violating the axiom.

5 Results

5.1 Locality

To illustrate the implication of the locality axiom, we analyzed the responses of a model neuron to a one-dimensional stimulus drawn from a Gaussian prior. The neuron's response was modeled as a Gaussian random variable with mean f(x) and fixed standard deviation. We compared two tuning curves: one with a single peak at x = -3 (Fig. 1A, black), and another with an additional peak at x = 6 (Fig. 1A, red).

With gaussian noise, Fisher information scales with $f'(x)^2$, and thus peaked where the tuning curves were steepest (Fig. 1B). Similar qualitative behaviour was observed for $I_{local}(x)$ (Fig 1C). Crucially, the difference in $I_{local}(x)$ between the two tuning curves vanished outside the region where they differ, consistent with the locality axiom. In contrast, existing attribution methods (Fig. 1D–G) showed global sensitivity: adding a second peak at x=6 altered the attributed information across the entire stimulus space, including far from the added feature.

5.2 Effect of Prior

We next examined how $I_{local}(x)$ responds to changes in the shape of the stimulus prior. For this, we considered two different stimulus priors: a zero-mean gaussian, and a bimodal mixture of two gaussians with peaks at x=-1 and x=1 (Fig. 2A-B, upper panels). To isolate the effect of the prior, we used a simple linear-Gaussian likelihood model: $r \sim \mathcal{N}(x, \sigma^2)$. Under this model, the neuron's sensitivity is uniform across all stimuli, so any variation in attributed information must arise solely from the prior.

Intuitively, one can assess neural sensitivity by measuring how much the posterior distribution $p(X \mid r)$ changes, on average, in response to small perturbations in the stimulus x. With the bimodal prior (Fig. 2B), the posterior is highly sensitive near x = 0, where the two modes compete (Fig. 2B,

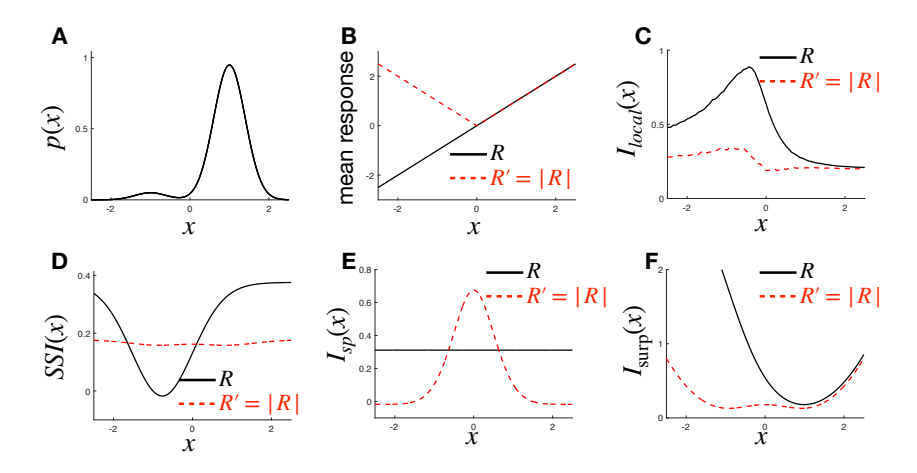


Figure 3: Local data processing inequality. (A) Bimodal prior. (B) Neural responses: r = x + noise; transformed response r' = |r|. The non-invertible transform reduces information. (C) Our decomposition satisfies the pointwise data processing inequality (DPI): $I_{R'}(x)$ (red) is always less than or equal to $I_R(x)$ (black). (D-F) I_{surp} also satisfies pointwise DPI, while I_{SSI} and I_{sp} do not. I_{CiSSI} (not shown) behaves similarly to I_{surp} .

middle panel), and relatively stable near the modes themselves, e.g., around x=1 (Fig. 2B, lower panel). Our attribution measure $I_{\rm local}(x)$ reflects this structure, peaking at x=0, and decaying elsewhere (Fig. 2C). For the Gaussian prior, where posterior sensitivity is constant, $I_{\rm local}(x)$ is flat. In contrast, previously proposed attribution methods behave inconsistently: some remain constant across both priors (Fig. 2D), others respond in the opposite direction (Fig. 2E), and some varied strongly even under a Gaussian prior, where the posterior sensitivity is uniform (Fig. 2F).

5.3 Data Processing Inequality

Next we illustrate how $I_{local}\left(x\right)$ respects the data processing inequality while certain other attribution methods do not. For this, we used a bimodal prior (Fig. 3A) and compared a linear-Gaussian neuron $(r \sim \mathcal{N}(x, \sigma_r^2))$ to a downstream neuron with response r' = |r|. Since this transformation is non-invertible, information must be lost. Consistent with the inequality, $I_{local}(x)$ decreased at every x (Fig 3C). In contrast, both I_{SSI} and I_{sp} increased at some x and decreased at others, violating the pointwise data processing inequality (Fi 3D-E). I_{surp} , by comparison, respected the inequality (Fig 3F).

5.4 Scaling to high-dimensions

We can use Eqn 20 to write the feature-wise decomposition in terms of the outputs of an unconditional and conditional diffusion model, trained to output $\hat{x}(x_{\gamma}) = E\left[X|x_{\gamma}\right]$ and $\hat{x}(x_{\gamma},r) = E\left[X|x_{\gamma},r\right]$, respectively:

$$I_i(x) = \int_0^\infty \frac{1}{2\gamma^2} \mathbb{E}_{X_\gamma|x,R|X_\gamma} \left[\left(\hat{x}_i(X_\gamma, R) - \hat{x}_i(X_\gamma) \right)^2 \right] d\gamma \tag{21}$$

To obtain a Monte-carlo approximation of this expression, we need to sample from $x_{\gamma} \sim p\left(X_{\gamma}|x\right)$, followed by, $r \sim p\left(R|x_{\gamma}\right)$. Sampling from $p\left(R|x_{\gamma}\right)$ is prohibitively expensive (since it requires first sampling from $x \sim p(x_{0}|x_{\gamma})$, which requires a full backward pass of the diffusion model). To get around this, we adopt an approximation used by Chung et al. 2023, instead approximating $I_{i}(x)$ using samples $r \sim p(R|\hat{x}\left(x\right))$, which can be computed efficiently using one pass through the de-noising network. The integral over γ was approximated numerically with evenly spaced γ (see Appendix C). Since the Fisher decays to zero for large γ , truncating the integral has little effect on our approximation of the integral.

5.5 Pixel-wise decomposition of encoded information

We applied our method to identify which regions of an image contribute most to the total information encoded by a population of visual neurons. For illustrative purposes, we used stimuli from the MNIST

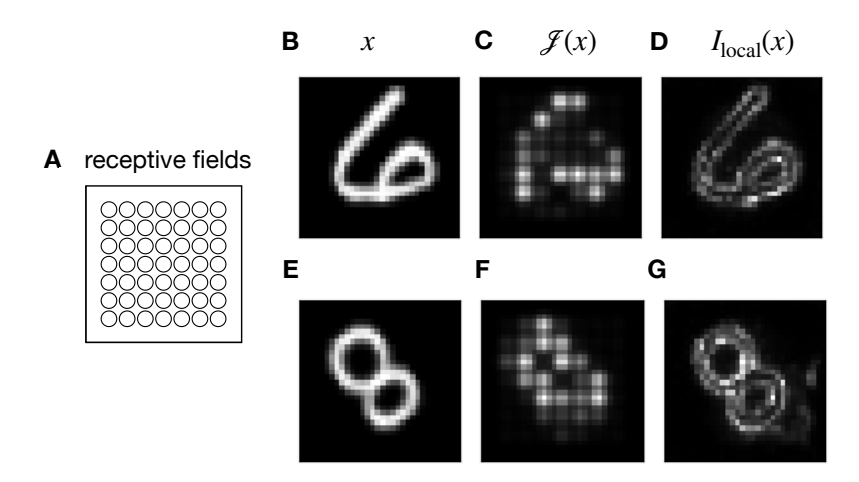


Figure 4: **Pixel-wise information decomposition with MNIST stimuli.** (A) Simulated population of linear–nonlinear–Poisson (LNP) neurons with circular receptive fields arranged in a grid. (B) Presented visual stimulus. (C) Diagonal of the Fisher information, given by a weighted sum of neural receptive fields. (D) Pixel-wise decomposition of mutual information, $I_{\rm local}(x)$. E-G Same as panels A-B, but for a different stimulus.

dataset and modelled a simple population of neurons with mean responses given by $Af(\mathbf{w} \cdot \mathbf{x} + b)$, where A and b are constants, $f(\cdot)$ is a sigmoid nonlinearity, and \mathbf{w} is a linear filter representing the neuron's receptive field (RF). Neural responses were corrupted by Poisson noise. We simulated 49 neurons with RFs arranged in a uniform grid (Fig. 4A).

As a baseline, we first evaluated neural sensitivity using the diagonal of the Fisher information matrix (Fig. 4B–C, E–F). In this model, the Fisher information reduces to a weighted sum of squared RFs, where each neuron's contribution is scaled by its activation level. This yields characteristic "blob-like" patterns, with each blob centered on the neuron's RF.

We then used a diffusion model trained on MNIST to estimate the pixel-wise information decomposition, $I_{\rm local}(\mathbf{x})$ (Fig 4D, G; additional images are shown in Supp Fig 2). This decomposition revealed that information was concentrated along object edges—regions where the decoded images (i.e. samples form the posterior) are most sensitive to small changes in the presented stimulus (cf. Fig. 2A). Unlike the Fisher information, our measure integrates how both the local sensitivity of neurons (via their RFs) and the statistical structure of the input (captured by the diffusion model), contribute towards the total encoded information.

Later, we investigated the behavior of our information decomposition on a diffusion model trained on natural images, with a model of recorded ganglion cell responses from the retina Klindt et al. [2017] (Appendix section C.6, and supplementary Figure 3). We observed qualitatively similar behavior to before, with I_{local} peaking in regions of high local spatial contrast, around the edges of objects.

6 Discussion

We introduced a principled, information-theoretic measure of neural sensitivity to stimuli. This measure satisfies a core set of axioms that ensure interpretability and theoretical soundness. Crucially, the measure can be estimated using diffusion models, making it scalable to high-dimensional inputs and complex, non-linear neural populations. We empirically demonstrated how each axiom shapes interpretability through simple, illustrative examples. Finally, we show how the method can be applied in a high-dimensional setting to quantify the information encoded by a neural population about visual stimuli.

Kong et al. 2024 recently proposed two decompositions of the mutual information between visual stimuli x and text prompts y, I(x,y), which can be efficiently estimated using diffusion models. These were used to identify image regions most informative about accompanying text. Dewan et al. 2024 extended this approach to assess pixel-wise redundancy and synergy with respect to the prompt. However, these frameworks do not directly yield a stimulus-wise neural sensitivity measure

I(x), which was our goal (Appendix B). Moreover, simply averaging the decompositions of Kong et al. over neural responses does not produce stimulus-wise and feature-wise decompositions that satisfy our axioms: in one case the resulting decomposition is non-local and can be negative; in the other case, the decomposition is not additive, and thus violates a key information theoretic property pointwise.

Our work extends a classical result from Brunel & Nadal 1998, who showed that mutual information can be approximated in the low-noise limit using Fisher information [Wei and Stocker, 2016]. This approximation was later used by Wei & Stocker 2015 to explain a wide range of perceptual phenomena under the efficient coding hypothesis [Morais and Pillow, 2018]. However, their approximation, which depends on the log determinant of the Fisher, becomes very inaccurate in certain cases, such as at high noise, or where there are more stimulus dimensions than neurons (in which case it returns minus infinity) [Bethge et al., 2002, Yarrow et al., 2012, Huang and Zhang, 2018]. Here, we instead identify an *exact* relation between mutual information and Fisher information with respect to a noise-corrupted stimulus. This opens new potential to test theories of efficient coding of high-dimensional stimuli, and in the presence of noise.

In the future, we will use our method to investigate more realistic neural models, fitted on biological data, as well as diffusion models trained on natural image datasets. Here, to further improve efficiency we could use zero-shot methods that sample directly from the posterior, without requiring a trained conditional diffusion model [Peng et al., 2024, Chung et al., 2023]. Such approaches have recently achieved state-of-the-art performance in decoding visual scenes from retinal ganglion cell responses [Wu et al., 2022], and could enable rapid assessment of how changes to the neural model affect encoded stimulus information.

Finally, our axiomatic framework has close parallels with integrated gradients [Sundararajan et al., 2017], a method developed to attribute the output of deep neural networks to individual input features. Both our method and integrated gradients address ill-posed attribution problems by enforcing natural axioms. However, one limitation of our method, in contrast to integrated gradients, is that we do not prove the uniqueness of our attribution method, as following from our axioms. This will be interesting to investigate in the future. There are also key differences between both approaches: for example, our attribution explicitly accounts for noisy responses and does not require specification of an arbitrary baseline. These distinctions make our method particularly well-suited to neural data, and suggest potential utility as a principled attribution tool for analyzing deep networks—identifying which stimuli, or stimulus features, different units or layers are sensitive to.

Acknowledgements

Ulisse Ferrari and Simone Azeglio acknowledge this work was done within the framework of the PostGenAI@Paris project with the reference ANR-23-IACL-0007. Ulisse Ferrari and Simone Azeglio benefited from financial support by the Agence Nationale de la Recherche (ANR) by grants NatNetNoise (ANR-21 CE37-0024), IHU FOReSIGHT (ANR-18-IAHU-01). The PhD position of Simone Azeglio was funded by the Sorbonne Center for Artificial Intelligence (SCAI), through IDEX Sorbonne Université, project reference ANR-11-IDEX-0004. Matthew Chalk and Steeve Laquitaine are funded by a grant RetNet4EC (ANR-22-CE92-0015), cofunded by the ANR and DFG. Our lab is part of the DIM C-BRAINS, funded by the Conseil Régional d'Île-de-France.

We would also like to thank Tobias Kuhn and Olivier Rioul for interesting discussion and input, which helped us towards this paper.

References

Matthias Bethge, David Rotermund, and Klaus Pawelzik. Optimal short-term population coding: When fisher information fails. *Neural computation*, 14(10):2317–2351, 2002.

Naama Brenner, Steven P Strong, Roland Koberle, William Bialek, and Rob R de Ruyter van Steveninck. Synergy in a neural code. *Neural computation*, 12(7):1531–1552, 2000.

Nicolas Brunel and Jean-Pierre Nadal. Mutual information, fisher information, and population coding. *Neural computation*, 10(7):1731–1757, 1998.

- Daniel A Butts. How much information is associated with a particular stimulus? *Network: Computation in Neural Systems*, 14(2):177, 2003.
- Daniel A Butts and Mark S Goldman. Tuning curves, neuronal variability, and sensory coding. *PLoS biology*, 4(4):e92, 2006.
- Hyungjin Chung, Jeongsol Kim, Michael Thompson Mccann, Marc Louis Klasky, and Jong Chul Ye. Diffusion posterior sampling for general noisy inverse problems. In *The Eleventh International Conference on Learning Representations*, 2023. URL https://openreview.net/forum?id=OnD9zGAGTOk.
- Shaurya Rajat Dewan, Rushikesh Zawar, Prakanshul Saxena, Yingshan Chang, Andrew Luo, and Yonatan Bisk. Diffusion PID: Interpreting diffusion via partial information decomposition. In *The Thirty-eighth Annual Conference on Neural Information Processing Systems*, 2024. URL https://openreview.net/forum?id=aBpxukZS37.
- Michael R DeWeese and Markus Meister. How to measure the information gained from one symbol. *Network: Computation in Neural Systems*, 10(4):325, 1999.
- Xuehao Ding, Dongsoo Lee, Joshua Melander, George Sivulka, Surya Ganguli, and Stephen Baccus. Information geometry of the retinal representation manifold. *Advances in Neural Information Processing Systems*, 36:44310–44322, 2023.
- MatÃas A. Goldin, Baptiste Lefebvre, Samuele Virgili, Mathieu Kim Pham Van Cang, Alexander Ecker, Thierry Mora, Ulisse Ferrari, and Olivier Marre. Context-dependent selectivity to natural images in the retina. *Nature Communications*, 13(1):5556, September 2022. ISSN 2041-1723. doi: 10.1038/s41467-022-33242-8. URL https://www.nature.com/articles/s41467-022-33242-8.
- Sylvain Gugger, Lysandre Debut, Thomas Wolf, Philipp Schmid, Zachary Mueller, Sourab Mangrulkar, Marc Sun, and Benjamin Bossan. Accelerate: Training and inference at scale made simple, efficient and adaptable. https://github.com/huggingface/accelerate, 2022.
- Jonathan Ho, Ajay Jain, and Pieter Abbeel. Denoising diffusion probabilistic models. *Advances in neural information processing systems*, 33:6840–6851, 2020.
- Wentao Huang and Kechen Zhang. Information-theoretic bounds and approximations in neural population coding. *Neural computation*, 30(4):885–944, 2018.
- Zahra Kadkhodaie and Eero P Simoncelli. Solving linear inverse problems using the prior implicit in a denoiser. *arXiv preprint arXiv:2007.13640*, 2020.
- David Klindt, Alexander S Ecker, Thomas Euler, and Matthias Bethge. Neural system identification for large populations separating "what" and "where". In I. Guyon, U. Von Luxburg, S. Bengio, H. Wallach, R. Fergus, S. Vishwanathan, and R. Garnett, editors, *Advances in Neural Information Processing Systems*, volume 30. Curran Associates, Inc., 2017. URL https://proceedings.neurips.cc/paper_files/paper/2017/file/8c249675aea6c3cbd91661bbae767ff1-Paper.pdf.
- Xianghao Kong, Ollie Liu, Han Li, Dani Yogatama, and Greg Ver Steeg. Interpretable diffusion via information decomposition. In *The Twelfth International Conference on Learning Representations*, 2024. URL https://openreview.net/forum?id=X6tNkN6ate.
- Lubomir Kostal and Giuseppe D'Onofrio. Coordinate invariance as a fundamental constraint on the form of stimulus-specific information measures. *Biological Cybernetics*, 112:13–23, 2018.
- Nikolaus Kriegeskorte and Xue-Xin Wei. Neural tuning and representational geometry. *Nature Reviews Neuroscience*, 22(11):703–718, 2021.
- Yann LeCun, Léon Bottou, Yoshua Bengio, and Patrick Haffner. Gradient-based learning applied to document recognition. *Proceedings of the IEEE*, 86(11):2278–2324, 1998.

- Chenlin Meng, Yang Song, Wenzhe Li, and Stefano Ermon. Estimating high order gradients of the data distribution by denoising. In A. Beygelzimer, Y. Dauphin, P. Liang, and J. Wortman Vaughan, editors, *Advances in Neural Information Processing Systems*, 2021. URL https://openreview.net/forum?id=YTkQQrqSyE1.
- Michael Morais and Jonathan W Pillow. Power-law efficient neural codes provide general link between perceptual bias and discriminability. *Advances in Neural Information Processing Systems*, 31, 2018.
- Xinyu Peng, Ziyang Zheng, Wenrui Dai, Nuoqian Xiao, Chenglin Li, Junni Zou, and Hongkai Xiong. Improving diffusion models for inverse problems using optimal posterior covariance, 2024. URL https://openreview.net/forum?id=9mXOAZVEet.
- C Radhakrishna Rao. Information and the accuracy attainable in the estimation of statistical parameters. In *Breakthroughs in Statistics: Foundations and basic theory*, pages 235–247. Springer, 1992.
- Olaf Ronneberger, Philipp Fischer, and Thomas Brox. U-net: Convolutional networks for biomedical image segmentation. In *Medical image computing and computer-assisted intervention–MICCAI* 2015: 18th international conference, Munich, Germany, October 5-9, 2015, proceedings, part III 18, pages 234–241. Springer, 2015.
- Claude E Shannon. A mathematical theory of communication. *The Bell system technical journal*, 27 (3):379–423, 1948.
- Mukund Sundararajan, Ankur Taly, and Qiqi Yan. Axiomatic attribution for deep networks. In *International conference on machine learning*, pages 3319–3328. PMLR, 2017.
- Patrick von Platen, Suraj Patil, Anton Lozhkov, Pedro Cuenca, Nathan Lambert, Kashif Rasul, Mishig Davaadorj, Dhruv Nair, Sayak Paul, William Berman, Yiyi Xu, Steven Liu, and Thomas Wolf. Diffusers: State-of-the-art diffusion models. https://github.com/huggingface/diffusers, 2022.
- Xue-Xin Wei and Alan A Stocker. A bayesian observer model constrained by efficient coding can explain'anti-bayesian'percepts. *Nature neuroscience*, 18(10):1509–1517, 2015.
- Xue-Xin Wei and Alan A Stocker. Mutual information, fisher information, and efficient coding. *Neural computation*, 28(2):305–326, 2016.
- Eric Wu, Nora Brackbill, Alexander Sher, Alan Litke, Eero Simoncelli, and EJ Chichilnisky. Maximum a posteriori natural scene reconstruction from retinal ganglion cells with deep denoiser priors. *Advances in Neural Information Processing Systems*, 35:27212–27224, 2022.
- Stuart Yarrow, Edward Challis, and Peggy Seriès. Fisher and shannon information in finite neural populations. *Neural computation*, 24(7):1740–1780, 2012.
- Ram Zamir. A proof of the fisher information inequality via a data processing argument. *IEEE Transactions on Information Theory*, 44(3):1246–1250, 1998.

NeurIPS Paper Checklist

1. Claims

Question: Do the main claims made in the abstract and introduction accurately reflect the paper's contributions and scope?

Answer: [Yes]

Justification: In the abstract and introduction we claim that we derive a new information theoretic decomposition based on principled axioms, We then illustrate its behavior on toy examples, as well as a high-d neural model. This is exactly what we do.

Guidelines:

- The answer NA means that the abstract and introduction do not include the claims made in the paper.
- The abstract and/or introduction should clearly state the claims made, including the contributions made in the paper and important assumptions and limitations. A No or NA answer to this question will not be perceived well by the reviewers.
- The claims made should match theoretical and experimental results, and reflect how much the results can be expected to generalize to other settings.
- It is fine to include aspirational goals as motivation as long as it is clear that these goals
 are not attained by the paper.

2. Limitations

Question: Does the paper discuss the limitations of the work performed by the authors?

Answer: [Yes]

Justification: We describe the limitations in the discussion. For example, one limitation is that we currently only consider simple neural models, and diffusion models of MNIST digits. In the future we will extend to more complex neural models and diffusion models trained on natural images. Another limitation is that we don't prove the uniqueness of our decomposition in fulfilling are axioms. This is also discussed.

Guidelines:

- The answer NA means that the paper has no limitation while the answer No means that the paper has limitations, but those are not discussed in the paper.
- The authors are encouraged to create a separate "Limitations" section in their paper.
- The paper should point out any strong assumptions and how robust the results are to violations of these assumptions (e.g., independence assumptions, noiseless settings, model well-specification, asymptotic approximations only holding locally). The authors should reflect on how these assumptions might be violated in practice and what the implications would be.
- The authors should reflect on the scope of the claims made, e.g., if the approach was only tested on a few datasets or with a few runs. In general, empirical results often depend on implicit assumptions, which should be articulated.
- The authors should reflect on the factors that influence the performance of the approach. For example, a facial recognition algorithm may perform poorly when image resolution is low or images are taken in low lighting. Or a speech-to-text system might not be used reliably to provide closed captions for online lectures because it fails to handle technical jargon.
- The authors should discuss the computational efficiency of the proposed algorithms and how they scale with dataset size.
- If applicable, the authors should discuss possible limitations of their approach to address problems of privacy and fairness.
- While the authors might fear that complete honesty about limitations might be used by reviewers as grounds for rejection, a worse outcome might be that reviewers discover limitations that aren't acknowledged in the paper. The authors should use their best judgment and recognize that individual actions in favor of transparency play an important role in developing norms that preserve the integrity of the community. Reviewers will be specifically instructed to not penalize honesty concerning limitations.

3. Theory assumptions and proofs

Question: For each theoretical result, does the paper provide the full set of assumptions and a complete (and correct) proof?

Answer: [Yes]

Justification: The main theoretical results are described in main body of the paper. Where space was limited we have included additional theoretical results in Appendix A and B.

Guidelines:

- The answer NA means that the paper does not include theoretical results.
- All the theorems, formulas, and proofs in the paper should be numbered and crossreferenced.
- All assumptions should be clearly stated or referenced in the statement of any theorems.
- The proofs can either appear in the main paper or the supplemental material, but if they appear in the supplemental material, the authors are encouraged to provide a short proof sketch to provide intuition.
- Inversely, any informal proof provided in the core of the paper should be complemented by formal proofs provided in appendix or supplemental material.
- Theorems and Lemmas that the proof relies upon should be properly referenced.

4. Experimental result reproducibility

Question: Does the paper fully disclose all the information needed to reproduce the main experimental results of the paper to the extent that it affects the main claims and/or conclusions of the paper (regardless of whether the code and data are provided or not)?

Answer: [Yes]

Justification: The information needed to reproduce the main results in the paper are described in the paper. Additional details, required to reproduce the neural model and diffusion model to reproduce figure 4 are provided in Appendix C. We also share our code on an anoymised github repository.

Guidelines:

- The answer NA means that the paper does not include experiments.
- If the paper includes experiments, a No answer to this question will not be perceived
 well by the reviewers: Making the paper reproducible is important, regardless of
 whether the code and data are provided or not.
- If the contribution is a dataset and/or model, the authors should describe the steps taken to make their results reproducible or verifiable.
- Depending on the contribution, reproducibility can be accomplished in various ways. For example, if the contribution is a novel architecture, describing the architecture fully might suffice, or if the contribution is a specific model and empirical evaluation, it may be necessary to either make it possible for others to replicate the model with the same dataset, or provide access to the model. In general, releasing code and data is often one good way to accomplish this, but reproducibility can also be provided via detailed instructions for how to replicate the results, access to a hosted model (e.g., in the case of a large language model), releasing of a model checkpoint, or other means that are appropriate to the research performed.
- While NeurIPS does not require releasing code, the conference does require all submissions to provide some reasonable avenue for reproducibility, which may depend on the nature of the contribution. For example
 - (a) If the contribution is primarily a new algorithm, the paper should make it clear how to reproduce that algorithm.
 - (b) If the contribution is primarily a new model architecture, the paper should describe the architecture clearly and fully.
 - (c) If the contribution is a new model (e.g., a large language model), then there should either be a way to access this model for reproducing the results or a way to reproduce the model (e.g., with an open-source dataset or instructions for how to construct the dataset).

(d) We recognize that reproducibility may be tricky in some cases, in which case authors are welcome to describe the particular way they provide for reproducibility. In the case of closed-source models, it may be that access to the model is limited in some way (e.g., to registered users), but it should be possible for other researchers to have some path to reproducing or verifying the results.

5. Open access to data and code

Question: Does the paper provide open access to the data and code, with sufficient instructions to faithfully reproduce the main experimental results, as described in supplemental material?

Answer: [Yes]

Justification: We are sharing our code on an anonymised github repository, here: https://anonymous.4open.science/r/neural-info-decompo-5BAF/.

Guidelines:

- The answer NA means that paper does not include experiments requiring code.
- Please see the NeurIPS code and data submission guidelines (https://nips.cc/public/guides/CodeSubmissionPolicy) for more details.
- While we encourage the release of code and data, we understand that this might not be possible, so "No" is an acceptable answer. Papers cannot be rejected simply for not including code, unless this is central to the contribution (e.g., for a new open-source benchmark).
- The instructions should contain the exact command and environment needed to run to reproduce the results. See the NeurIPS code and data submission guidelines (https://nips.cc/public/guides/CodeSubmissionPolicy) for more details.
- The authors should provide instructions on data access and preparation, including how
 to access the raw data, preprocessed data, intermediate data, and generated data, etc.
- The authors should provide scripts to reproduce all experimental results for the new proposed method and baselines. If only a subset of experiments are reproducible, they should state which ones are omitted from the script and why.
- At submission time, to preserve anonymity, the authors should release anonymized versions (if applicable).
- Providing as much information as possible in supplemental material (appended to the paper) is recommended, but including URLs to data and code is permitted.

6. Experimental setting/details

Question: Does the paper specify all the training and test details (e.g., data splits, hyperparameters, how they were chosen, type of optimizer, etc.) necessary to understand the results?

Answer: [Yes]

Justification: The diffusion model used to reproduce the final figure was taken directly from a previous paper without modification. Training details are described in Appendix C, along with the neural model.

Guidelines:

- The answer NA means that the paper does not include experiments.
- The experimental setting should be presented in the core of the paper to a level of detail that is necessary to appreciate the results and make sense of them.
- The full details can be provided either with the code, in appendix, or as supplemental material.

7. Experiment statistical significance

Question: Does the paper report error bars suitably and correctly defined or other appropriate information about the statistical significance of the experiments?

Answer: [NA]

Justification: The simulations used in the paper were used to illustrate simple concepts, and did thus not require error bars.

Guidelines:

- The answer NA means that the paper does not include experiments.
- The authors should answer "Yes" if the results are accompanied by error bars, confidence intervals, or statistical significance tests, at least for the experiments that support the main claims of the paper.
- The factors of variability that the error bars are capturing should be clearly stated (for example, train/test split, initialization, random drawing of some parameter, or overall run with given experimental conditions).
- The method for calculating the error bars should be explained (closed form formula, call to a library function, bootstrap, etc.)
- The assumptions made should be given (e.g., Normally distributed errors).
- It should be clear whether the error bar is the standard deviation or the standard error
 of the mean.
- It is OK to report 1-sigma error bars, but one should state it. The authors should preferably report a 2-sigma error bar than state that they have a 96% CI, if the hypothesis of Normality of errors is not verified.
- For asymmetric distributions, the authors should be careful not to show in tables or figures symmetric error bars that would yield results that are out of range (e.g. negative error rates).
- If error bars are reported in tables or plots, The authors should explain in the text how they were calculated and reference the corresponding figures or tables in the text.

8. Experiments compute resources

Question: For each experiment, does the paper provide sufficient information on the computer resources (type of compute workers, memory, time of execution) needed to reproduce the experiments?

Answer: [Yes]

Justification: We specify the computing resources required for the diffusion model in Appendix C.

Guidelines:

- The answer NA means that the paper does not include experiments.
- The paper should indicate the type of compute workers CPU or GPU, internal cluster, or cloud provider, including relevant memory and storage.
- The paper should provide the amount of compute required for each of the individual experimental runs as well as estimate the total compute.
- The paper should disclose whether the full research project required more compute than the experiments reported in the paper (e.g., preliminary or failed experiments that didn't make it into the paper).

9. Code of ethics

Question: Does the research conducted in the paper conform, in every respect, with the NeurIPS Code of Ethics https://neurips.cc/public/EthicsGuidelines?

Answer: [Yes]

Justification: The authors have reviewed the NeurIPS Code of Ethics and confirmed that their paper, which includes mostly theoretical results, does not violate the code.

Guidelines:

- The answer NA means that the authors have not reviewed the NeurIPS Code of Ethics.
- If the authors answer No, they should explain the special circumstances that require a
 deviation from the Code of Ethics.
- The authors should make sure to preserve anonymity (e.g., if there is a special consideration due to laws or regulations in their jurisdiction).

10. Broader impacts

Question: Does the paper discuss both potential positive societal impacts and negative societal impacts of the work performed?

Answer: [NA]

Justification: The authors could not envisage a direct or indirect path to negative applications from this research.

Guidelines:

- The answer NA means that there is no societal impact of the work performed.
- If the authors answer NA or No, they should explain why their work has no societal impact or why the paper does not address societal impact.
- Examples of negative societal impacts include potential malicious or unintended uses (e.g., disinformation, generating fake profiles, surveillance), fairness considerations (e.g., deployment of technologies that could make decisions that unfairly impact specific groups), privacy considerations, and security considerations.
- The conference expects that many papers will be foundational research and not tied to particular applications, let alone deployments. However, if there is a direct path to any negative applications, the authors should point it out. For example, it is legitimate to point out that an improvement in the quality of generative models could be used to generate deepfakes for disinformation. On the other hand, it is not needed to point out that a generic algorithm for optimizing neural networks could enable people to train models that generate Deepfakes faster.
- The authors should consider possible harms that could arise when the technology is being used as intended and functioning correctly, harms that could arise when the technology is being used as intended but gives incorrect results, and harms following from (intentional or unintentional) misuse of the technology.
- If there are negative societal impacts, the authors could also discuss possible mitigation strategies (e.g., gated release of models, providing defenses in addition to attacks, mechanisms for monitoring misuse, mechanisms to monitor how a system learns from feedback over time, improving the efficiency and accessibility of ML).

11. Safeguards

Question: Does the paper describe safeguards that have been put in place for responsible release of data or models that have a high risk for misuse (e.g., pretrained language models, image generators, or scraped datasets)?

Answer: [NA]

Justification: The paper poses no such risks.

Guidelines:

- The answer NA means that the paper poses no such risks.
- Released models that have a high risk for misuse or dual-use should be released with
 necessary safeguards to allow for controlled use of the model, for example by requiring
 that users adhere to usage guidelines or restrictions to access the model or implementing
 safety filters.
- Datasets that have been scraped from the Internet could pose safety risks. The authors should describe how they avoided releasing unsafe images.
- We recognize that providing effective safeguards is challenging, and many papers do not require this, but we encourage authors to take this into account and make a best faith effort.

12. Licenses for existing assets

Question: Are the creators or original owners of assets (e.g., code, data, models), used in the paper, properly credited and are the license and terms of use explicitly mentioned and properly respected?

Answer: [Yes]

Justification: We used a diffusion model in the paper which was fully cited.

Guidelines:

- The answer NA means that the paper does not use existing assets.
- The authors should cite the original paper that produced the code package or dataset.

- The authors should state which version of the asset is used and, if possible, include a URL.
- The name of the license (e.g., CC-BY 4.0) should be included for each asset.
- For scraped data from a particular source (e.g., website), the copyright and terms of service of that source should be provided.
- If assets are released, the license, copyright information, and terms of use in the package should be provided. For popular datasets, paperswithcode.com/datasets has curated licenses for some datasets. Their licensing guide can help determine the license of a dataset.
- For existing datasets that are re-packaged, both the original license and the license of the derived asset (if it has changed) should be provided.
- If this information is not available online, the authors are encouraged to reach out to the asset's creators.

13. New assets

Question: Are new assets introduced in the paper well documented and is the documentation provided alongside the assets?

Answer: [NA]

Justification: while we share our code, there is not really a new asset emerging from this paper.

Guidelines:

- The answer NA means that the paper does not release new assets.
- Researchers should communicate the details of the dataset/code/model as part of their submissions via structured templates. This includes details about training, license, limitations, etc.
- The paper should discuss whether and how consent was obtained from people whose asset is used.
- At submission time, remember to anonymize your assets (if applicable). You can either create an anonymized URL or include an anonymized zip file.

14. Crowdsourcing and research with human subjects

Question: For crowdsourcing experiments and research with human subjects, does the paper include the full text of instructions given to participants and screenshots, if applicable, as well as details about compensation (if any)?

Answer: [NA]

Justification: The paper does not involve crowdsourcing.

Guidelines:

- The answer NA means that the paper does not involve crowdsourcing nor research with human subjects.
- Including this information in the supplemental material is fine, but if the main contribution of the paper involves human subjects, then as much detail as possible should be included in the main paper.
- According to the NeurIPS Code of Ethics, workers involved in data collection, curation, or other labor should be paid at least the minimum wage in the country of the data collector.

15. Institutional review board (IRB) approvals or equivalent for research with human subjects

Question: Does the paper describe potential risks incurred by study participants, whether such risks were disclosed to the subjects, and whether Institutional Review Board (IRB) approvals (or an equivalent approval/review based on the requirements of your country or institution) were obtained?

Answer: [NA]

Justification: The paper does not involve crowdsourcing nor research with human subjects Guidelines:

- The answer NA means that the paper does not involve crowdsourcing nor research with human subjects.
- Depending on the country in which research is conducted, IRB approval (or equivalent) may be required for any human subjects research. If you obtained IRB approval, you should clearly state this in the paper.
- We recognize that the procedures for this may vary significantly between institutions and locations, and we expect authors to adhere to the NeurIPS Code of Ethics and the guidelines for their institution.
- For initial submissions, do not include any information that would break anonymity (if applicable), such as the institution conducting the review.

16. Declaration of LLM usage

Question: Does the paper describe the usage of LLMs if it is an important, original, or non-standard component of the core methods in this research? Note that if the LLM is used only for writing, editing, or formatting purposes and does not impact the core methodology, scientific rigorousness, or originality of the research, declaration is not required.

Answer: [NA]

Justification: The core method development in this research does not involve LLMs as any important, original, or non-standard components.

Guidelines:

- The answer NA means that the core method development in this research does not involve LLMs as any important, original, or non-standard components.
- Please refer to our LLM policy (https://neurips.cc/Conferences/2025/LLM) for what should or should not be described.

A Proof of locality axiom

Let p(R, X) and $\tilde{p}(R, X)$ be two joint distributions, defined over the response, R, and a stimulus, X with infinite support in an unbounded (e.g. $X \in \mathbb{R}^d$) or semi-bounded domain (e.g. $[0, \infty)^d$).

We restrict $\tilde{p}(R, X)$ to only differ from p(R, X) locally, in the vicinity of x_0 . Formally, we suppose there exists finite $\epsilon > 0$ and x_0 such that:

$$p(R, x) = \tilde{p}(R, x)$$
 for all $x \notin B_{\epsilon}(x_0)$, (22)

where $B_{\epsilon}(x_0)$ is the open ball of radius ϵ centered at x_0 .

Recall that our stimulus-wise decomposition of information is defined as:

$$I(x) = \frac{1}{2} \operatorname{Trace} \int_0^\infty \mathbb{E}_{p(X_\gamma | x)} \left[\mathcal{J}(X_\gamma) \right] \, d\gamma, \tag{23}$$

where $X_{\gamma} = x + \sqrt{\gamma}Z$, $Z \sim \mathcal{N}(0, I)$, and $\mathcal{J}(x_{\gamma}) = \mathbb{E}_{p(R|x_{\gamma})} \left[-\nabla_{x_{\gamma}}^{2} \log p(R \mid x_{\gamma}) \right]$ is the Fisher information matrix at x_{γ} .

We will consider the absolute difference between the stimulus-wise information, computed with p(r,x) and $\tilde{p}(r,x)$ respectively, $|I(x)-\tilde{I}(x)|$. To prove the locality axiom, we separate the integral over γ into two parts as follows,

$$|I(x) - \tilde{I}(x)| = \frac{1}{2} \left| \text{Trace} \int_{0}^{\infty} \mathbb{E}_{p(X_{\gamma}|x)} \left[\mathcal{J}(X_{\gamma}) - \tilde{\mathcal{J}}(X_{\gamma}) \right] d\gamma \right|$$
 (24)

$$\leq f(x,\gamma_h) + g(x,\gamma_h),$$
 (25)

where

$$f(x, \gamma_h) = \frac{1}{2} \left| \text{Trace} \int_0^{\gamma_h} \mathbb{E}_{p(X_\gamma | x)} \left[\mathcal{J}(X_\gamma) - \tilde{\mathcal{J}}(X_\gamma) \right] d\gamma \right|$$
 (26)

$$g(x, \gamma_h) = \frac{1}{2} \left| \text{Trace} \int_{\gamma_h}^{\infty} \mathbb{E}_{p(X_{\gamma}|x)} \left[\mathcal{J}(X_{\gamma}) - \tilde{\mathcal{J}}(X_{\gamma}) \right] d\gamma \right|.$$
 (27)

In sections A.1, and A.2 we show that $f(x, \gamma_h)$ and $g(x, \gamma_h)$ have the following limiting behavior:

$$f(x, \gamma_h) = \mathcal{O}\left(e^{-\frac{1}{4\gamma_h}\|x - x_0\|^2}\right) \quad \text{as } \|x - x_0\|^2 \to \infty$$
 (28)

$$g(x, \gamma_h) = \mathcal{O}\left(\frac{1}{\gamma_h}\right) \text{ uniformly over } x \text{ as } \gamma_h \to \infty.$$
 (29)

Thus, for any $\delta > 0$, we can first pick γ_h large enough so that $g(x, \gamma_h) \leq \delta/2$, for all x. Then, for fixed γ_h , we choose d such that $f(x, \gamma_h) \leq \delta/2$ whenever $||x - x_0||^2 \geq d$.

This guarantees that for any $\delta > 0$, there exists a finite constant d such that,

$$|I(x) - \tilde{I}(x)| \le \delta$$
 for all $||x - x_0||^2 \ge d$, (30)

completing our proof of the locality axiom.

A.1 Integral from $\gamma = 0$ to $\gamma = \gamma_h$

Here, we prove the limiting behavior of $f(x, \gamma_h)$, as $||x - x_0||^2 \to \infty$.

We start by writing out the Fisher information as a function of the noise-corrupted stimulus, x_{γ} :

$$\operatorname{Trace}(\mathcal{J}(x_{\gamma})) = \frac{1}{\gamma^{2}} E_{R|x_{\gamma}} \left(\|\hat{x}(x_{\gamma}) - \hat{x}(x_{\gamma}, r)\|^{2} \right)$$
(31)

Writing out $\hat{x}(x_{\gamma}) \equiv E[X|x_{\gamma}]$ explicitly,

$$\hat{x}(x_{\gamma}) = \frac{\int x' p(x') \,\phi\left(\frac{x_{\gamma} - x'}{\sqrt{\gamma}}\right) dx'}{\int p(x') \,\phi\left(\frac{x_{\gamma} - x'}{\sqrt{\gamma}}\right) dx'}$$
(32)

$$= \frac{\int_{x' \notin B_{\epsilon}(x_0)} x' p(x') \phi\left(\frac{x' - x_{\gamma}}{\sqrt{\gamma}}\right) dx' + \int_{x' \in B_{\epsilon}(x_0)} x' p(x') \phi\left(\frac{x' - x_{\gamma}}{\sqrt{\gamma}}\right) dx'}{\int_{x' \notin B_{\epsilon}(x_0)} p(x') \phi\left(\frac{x' - x_{\gamma}}{\sqrt{\gamma}}\right) dx' + \int_{x' \in B_{\epsilon}(x_0)} p(x') \phi\left(\frac{x' - x_{\gamma}}{\sqrt{\gamma}}\right) dx'},$$
(33)

where $\phi(x) \equiv \frac{1}{\sqrt{2\pi}} e^{-\frac{1}{2}|x|^2}$, and we have separated the integrals in the numerator and denominator into contributions from inside and outside the region $B_{\epsilon}(x_0)$. Taking just the second term in the numerator of Eqn 33,

$$\int_{x' \in B_{\epsilon}(x_{0})} x' p(x') \phi\left(\frac{x' - x_{\gamma}}{\sqrt{\gamma}}\right) dx' \leq \sup_{x' \in B_{\epsilon}(x_{0})} \phi\left(\frac{x' - x_{\gamma}}{\sqrt{\gamma}}\right) \int_{x' \in B_{\epsilon}(x_{0})} x' p(x') dx'$$

$$= \phi\left(\frac{\|x_{0} - x_{\gamma}\| - \epsilon}{\sqrt{\gamma}}\right) \int_{x' \in B_{\epsilon}(x_{0})} x' p(x') dx'$$

$$= O\left(e^{-\frac{1}{2\gamma}\|x_{0} - x_{\gamma}\|^{2}}\right) \text{ as } \|x_{0} - x_{\gamma}\|^{2} \to \infty \quad (34)$$

since, by construction, p(x) has finite moments. The same logic also applies to the second term in the denominator of Eqn 33,

$$\int_{x' \in B_{\epsilon}(x_0)} p(x') \, \phi\left(\frac{x' - x_{\gamma}}{\sqrt{\gamma}}\right) dx' = \mathcal{O}(e^{-\frac{1}{2\gamma} \|x_0 - x_{\gamma}\|^2}) \quad \text{as} \quad \|x_0 - x_{\gamma}\|^2 \to \infty.$$
 (35)

Substituting this asymptotic behaviour back into Eqn 33, we have

$$\hat{x}(x_{\gamma}) = \frac{\int_{x' \notin B_{\epsilon}(x_0)} x' p(x') \phi\left(\frac{x' - x_{\gamma}}{\sqrt{\gamma}}\right) dx'}{\int_{x' \notin B_{\epsilon}(x_0)} p(x') \phi\left(\frac{x' - x_{\gamma}}{\sqrt{\gamma}}\right) dx'} + \mathcal{O}(e^{-\frac{1}{2\gamma} \|x_0 - x_{\gamma}\|^2})$$
(36)

where the first term only depends on x in the region outside the region $B_{\epsilon}(x_0)$.

Using the same arguments for $\hat{x}(x_{\gamma}, r)$, we can write:

$$\hat{x}(x_{\gamma}) - \hat{x}(x_{\gamma}, r) = a(x_{\gamma}, r, x_0) + \mathcal{O}(e^{-\frac{1}{2\gamma} \|x_0 - x_{\gamma}\|^2}), \tag{37}$$

where

$$a(x_{\gamma}, r, x_{0}) \equiv \frac{\int_{x' \notin B_{\epsilon}(x_{0})} x' p(x') \phi\left(\frac{x' - x_{\gamma}}{\sqrt{\gamma}}\right) dx'}{\int_{x' \notin B_{\epsilon}(x_{0})} p(x') \phi\left(\frac{x' - x_{\gamma}}{\sqrt{\gamma}}\right) dx'} - \frac{\int_{x' \notin B_{\epsilon}(x_{0})} x' p(r, x') \phi\left(\frac{x' - x_{\gamma}}{\sqrt{\gamma}}\right) dx'}{\int_{x' \notin B_{\epsilon}(x_{0})} p(r, x') \phi\left(\frac{x' - x_{\gamma}}{\sqrt{\gamma}}\right) dx'},$$
(38)

only depends on p(r, x) in the region $x \notin B_{\epsilon}(x_0)$.

Taking the square, and averaging over $p(r|x_{\gamma})$, we have

$$\operatorname{Trace}(\mathcal{J}(x_{\gamma})) = \frac{1}{\gamma^{2}} E_{R|x_{\gamma}} \left[\|a(x_{\gamma}, r, x_{0})\|^{2} \right] + \mathcal{O}(e^{-\frac{1}{2\gamma} \|x_{0} - x_{\gamma}\|^{2}})$$
(39)

$$= \frac{1}{\gamma^2} \frac{\int_{x,r} p(r|x)p(x)\phi\left(\frac{x-x_{\gamma}}{\sqrt{\gamma}}\right) \|a(x_{\gamma},r,x_0)\|^2 dx}{\int_x p(x)\phi\left(\frac{x-x_{\gamma}}{\sqrt{\gamma}}\right) dx} + \mathcal{O}(e^{-\frac{1}{2\gamma}\|x_0-x_{\gamma}\|^2})$$
(40)

Note that if R is discrete, the above integral over R is simply replaced by a sum. We then follow the exact same procedure as before, separating the integrals over x into parts that are inside and outside of $B_{\epsilon}(x_0)$, to obtain

Trace
$$(\mathcal{J}(x_{\gamma})) = \frac{1}{\gamma^2} ||b(x_{\gamma}, x_0)||^2 + \mathcal{O}(e^{-\frac{1}{2\gamma} ||x_0 - x_{\gamma}||})$$
 (41)

where $b(x_0, x_\gamma)$ is a function that only depends on p(r, x) in the region $x \notin B_{\epsilon}(x_0)$.

Since, by construction $\tilde{p}(r,x) = p(r,x)$ in the region $x \notin B_{\epsilon}(x_0)$, we can then write:

Trace
$$\left(\mathcal{J}(x_{\gamma}) - \tilde{\mathcal{J}}(x_{\gamma})\right) = \mathcal{O}(e^{-\frac{1}{2\gamma}\|x_0 - x_{\gamma}\|}), \quad \text{as } \|x_0 - x_{\gamma}\|^2 \to \infty$$
 (42)

where $\tilde{\mathcal{J}}(x_{\gamma})$ is the Fisher information obtained with $\tilde{p}(r,x)$.

Averaging over $p(X_{\gamma}|x) = \phi\left(\frac{X_{\gamma}-x}{\sqrt{\gamma}}\right)$ gives:

$$\mathbb{E}_{p(X_{\gamma}|x)} \left[\operatorname{Trace}(\mathcal{J}(x_{\gamma}) - \tilde{\mathcal{J}}(x_{\gamma})) \right] = \mathcal{O}\left(e^{-\frac{1}{4\gamma} \|x_0 - x\|^2} \right), \quad \text{as } \|x - x_0\|^2 \to \infty.$$
 (43)

Finally, integrating from $\gamma = 0$ to γ_h , we have:

$$f(x,\gamma_h) = \frac{1}{2} \left| \int_0^{\gamma_h} \text{Trace} \left(\mathbb{E}_{X_\gamma \mid x} \left[\mathcal{J}(X_\gamma) - \tilde{\mathcal{J}}(X_\gamma) \right] \right) d\gamma \right|$$
(44)

$$\leq \frac{1}{2} \int_{0}^{\gamma_{h}} \left| \operatorname{Trace} \left(\mathbb{E}_{X_{\gamma}|x} \left[\mathcal{J}(X_{\gamma}) - \tilde{\mathcal{J}}(X_{\gamma}) \right] \right) \right| d\gamma \tag{45}$$

$$\leq \frac{1}{2} \gamma_h \sup_{\gamma \in (0, \gamma_h)} \left| \operatorname{Trace} \left(\mathbb{E}_{X_{\gamma}|x} \left[\mathcal{J}(X_{\gamma}) - \tilde{\mathcal{J}}(X_{\gamma}) \right] \right) \right| \tag{46}$$

$$= \mathcal{O}\left(e^{-\frac{1}{4\gamma_h}\|x - x_0\|^2}\right) \text{ as } \|x - x_0\|^2 \to \infty, \tag{47}$$

as stated in Eqn 28.

A.2 Integral from $\gamma = \gamma_h$ to ∞

Next, we show the limiting behaviour of $g(x, \gamma_h)$.

We know from Eqn 42 that for any given $\gamma < \infty$, $|\operatorname{Trace}(\mathcal{J}(x_{\gamma}) - \tilde{\mathcal{J}}(x_{\gamma}))| \to 0$ as $|x_{\gamma}| \to \infty$. Thus the maximum of $|\operatorname{Trace}(\mathcal{J}(x_{\gamma}) - \tilde{\mathcal{J}}(x_{\gamma}))|$ must be obtained for some finite x_{γ}^* . As a result

$$|\operatorname{Trace}(\mathcal{J}(x_{\gamma}) - \tilde{\mathcal{J}}(x_{\gamma}))| \le \sup_{x_{\gamma}} |\operatorname{Trace}(\mathcal{J}(x_{\gamma}) - \tilde{\mathcal{J}}(x_{\gamma}))|$$
 (48)

$$= |\operatorname{Trace}(\mathcal{J}(x_{\gamma}^{*}) - \tilde{\mathcal{J}}(x_{\gamma}^{*}))|, \quad \text{where } |x_{\gamma}^{*}| < \infty$$

$$= \frac{1}{\gamma^{2}} \left| E_{p(r|x_{\gamma}^{*})} \left(\|\hat{x}(x_{\gamma}^{*}) - \hat{x}\left(x_{\gamma}^{*}, r\right)\|^{2} \right)$$

$$(49)$$

$$-E_{\tilde{p}(r|x_{\gamma}^{*})}\left(\|\tilde{x}(x_{\gamma}^{*}) - \tilde{x}\left(x_{\gamma}^{*}, r\right)\|^{2}\right), \quad \text{where } |x_{\gamma}^{*}| < \infty \quad (50)$$

with $\tilde{x}(x_{\gamma})$ and $\tilde{x}(x_{\gamma},r)$ defined as the expectations over X obtained with the perturbed distribution, $\tilde{p}(R,X)$. Now since, by construction, p(x), $p(x\mid r)$, $\tilde{p}(x)$, and $\tilde{p}(x\mid r)$ all have finite first and second moments, then for finite x_{γ}^{*} all the expectations in the above expression are finite, and we have:

$$|\operatorname{Trace}(\mathcal{J}(x_{\gamma}) - \tilde{\mathcal{J}}(x_{\gamma}))| \le \frac{C}{\gamma^2}, \quad \text{ for all } x_{\gamma}$$
 (51)

where $C < \infty$ is some finite constant, independent of x_{γ} .

Integrating over γ and averaging over $p(X_{\gamma}|x)$ gives

$$g(x, \gamma_h) = \frac{1}{2} \left| \text{Trace} \int_{\gamma_h}^{\infty} \mathbb{E}_{X_{\gamma}|x} \left[\mathcal{J}(X_{\gamma}) - \tilde{\mathcal{J}}(X_{\gamma}) \right] d\gamma \right|$$
 (52)

$$\leq \frac{1}{2} \int_{\gamma_h}^{\infty} \left| \mathbb{E}_{X_{\gamma}|x} \left[\operatorname{Trace} \left(\mathcal{J}(X_{\gamma}) - \tilde{\mathcal{J}}(X_{\gamma}) \right) \right] \right| d\gamma \tag{53}$$

$$\leq \frac{C}{2\gamma_h}, \quad \text{for all } x$$
 (54)

$$= \mathcal{O}\left(\frac{1}{\gamma_h}\right), \quad \text{uniformly in } x, \tag{55}$$

as stated in Eqn 29.

B Comparison with previous decompositions using diffusion models

Recently Kong et al. 2024 proposed two different decompositions of the mutual information into terms that depend on both the response and stimulus, which can be computed using diffusion models. Their decompositions take the following form:

$$I_{Kong,1}(x,r) = \int_0^\infty \frac{1}{2\gamma^2} E_{X_\gamma|x} \left[\|x - \hat{x}(x_\gamma, r)\|^2 - \|x - \hat{x}(x_\gamma)\|^2 \right] d\gamma$$
 (56)

$$I_{Kong,2}(x,r) = \int_0^\infty \frac{1}{2\gamma^2} E_{X_{\gamma}|x} \left[\|\hat{x}(x_{\gamma}) - \hat{x}(x_{\gamma},r)\|^2 \right] d\gamma$$
 (57)

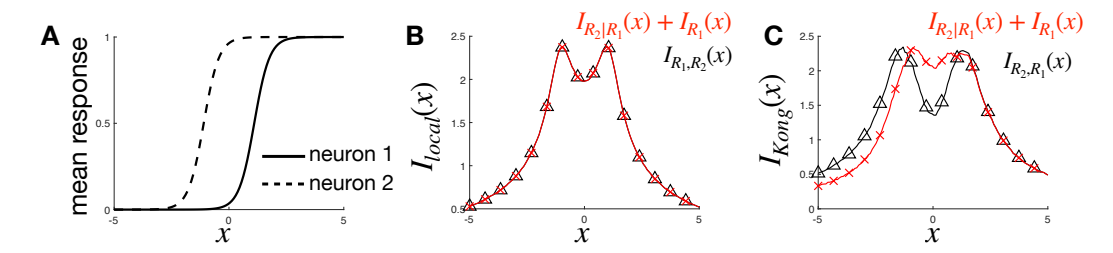


Figure 5: Additivity, with respect to measurements from multiple neurons. (A) We considered two neurons, with sigmoidal tuning curves, f(x), and a 1-d stimulus with gaussian prior. (B) We confirmed that $I_{local}(x)$ satisfies additivity, by checking that the point-wise information from both neurons together $(I_{R,R_2}(x), \text{red})$ equals $I_{R_1}(x) + I_{R_2|R_1}(x)$. (C) For the measure derived from the work of Kong et al., which does not satisfy additivity, the curves are non-overlapping.

To obtain stimulus-wise decompositions from these expressions, that we can compare with our work, we averaged both of these decompositions with respect to p(R|x), to obtain: $I_{Kong,1}(x) \equiv \mathbb{E}_{R|x}\left[I_{Kong,1}(x,R)\right]$ and $I_{Kong,2}(x) \equiv \mathbb{E}_{R|x}\left[I_{Kong,2}(x,R)\right]$.

Despite the apparent similarity with our proposed decomposition, neither $I_{Kong,1}(x)$ or $I_{Kong,2}(x)$ fulfill our axioms, limiting their potential use as principled & interpretable measures of neural sensitivity.

In their paper, Kong et al. show that $I_{Kong,1}(x,r) = \log \frac{p(r|x)}{p(r)}$. Taking the average over p(R|x), gives: $I_{Kong,1}(x) \equiv \mathbb{E}_{R|x}\left[I_{Kong,1}(x,r)\right] = D_{KL}(p(R|x)||p(R))$. This is identical to the expression for the specific surprise, $I_{surp}(x)$, in the main text (Eqn 3). As shown in the main text (Fig 1E), this measure does not fulfill our locality axiom. This is because $I_{surp}(x)$ depends on $p(r) = \int p(r|x')p(r')dx'$, which can be influenced by changes to the likelihood or prior with respect to any stimulus, x'. Further, following the same prescription as in the main text to obtain a feature-wise decomposition of $I_{Kong,1}(x)$, results in feature-wise attributions that can be negative.

To understand the second decomposition, we use Tweedie's law to write:

$$I_{Kong,2}(x) \equiv \mathbb{E}_{R|x} \left[I_{Kong,2}(x,r) \right] = \frac{1}{2} \int_0^\infty \mathbb{E}_{X_\gamma,R|x} \left[\| \nabla_{x_\gamma} \log p(R|X_\gamma) \|^2 \right] d\gamma \tag{58}$$

This differs from our expression, due to the fact that it involves taking the average over p(R|x), rather than $p(R|x_{\gamma})$. However, while this difference may seem subtle it has important consequences for the resulting stimulus-wise decomposition.

To see that there are large qualitative differences between $I_{Kong,2}(x)$ and $I_{local}(x)$ we first consider their behavior in the case where p(R,X) is jointly gaussian. Here, $I_{local}(x)$ is constant across x (Fig 2B, black), reflecting that the fact that the posterior is also independent of x (up to a linear translation). In contrast, $I_{Kong,2}(x)$ scales quadratically with the distance of x from the mean (similar to $I_{surp}(x)$, Fig 2E).

More importantly, $I_{\text{Kong},2}(x)$ violates **additivity** point-wise. Supp Fig 1 illustrates this in a simple 1-d example. To see why it is the case, we can expand the expression for the local information from two neurons, R and R':

$$I_{R,R'}^{Kong,2}(x) = \frac{1}{2} \int_0^\infty \mathbb{E}_{X_{\gamma},R,R'|x} \left[\|\nabla_{x_{\gamma}} \log p(R'|R,X_{\gamma}) + \nabla_{x_{\gamma}} \log p(R|X_{\gamma}) \|^2 \right] d\gamma$$
 (59)

Now when we expand the square we see that the cross-terms *don't cancel out*. As a result, $I_{Kong,2}$ is not linear in $\log p(R'|R, X_{\gamma})$ and $\log p(R|X_{\gamma})$, violating additivity.

This contrasts with the behaviour of I_{local} , which can be expressed as follows:

$$I_{R,R'}^{local}(x) = -\frac{1}{2} \int_0^\infty \mathbb{E}_{X_\gamma|x} \left\{ \mathbb{E}_{R',R|X_\gamma} \left[\nabla_{x_\gamma}^2 \log p(R'|R,X_\gamma) + \nabla_{x_\gamma}^2 \log p(R|X_\gamma) \right] \right\} d\gamma \quad (60)$$

This equation is linear in $\log p(R'|R, X_{\gamma})$ and $\log p(R|X_{\gamma})$, and thus we can easily confirm that it is additive with respect to repeated measurements.

Additivity is a fundamental property that underpins the definition of mutual information [Shannon, 1948]. It requires that information from multiple measurements (e.g., different neurons) combine linearly, such that their individual contributions sum to the total local information (Fig. 5). A pointwise measure that doesn't respect additivity could thus lead to misleading attributions as they don't respect how different measurements (or neurons) combine additively to generate the total mutual information.

C Diffusion model details

C.1 Dataset Preparation

We utilized the MNIST dataset LeCun et al. [1998], which consists of 60,000 grayscale images of handwritten digits for training and 10,000 for testing. Each image, originally 28×28 pixels, was preprocessed by normalizing to the range [-1,1] and then rescaled to 32×32 pixels to align with the architectural requirements of our diffusion models.

C.2 Neural Encoding Model

We simulated a population of 49 neurons with spatially localized receptive fields (RFs) arranged in a 7×7 grid, mimicking the retinotopic organization of early visual cortex. Image pixels were mapped to 2D coordinates in visual space, $(x, y) \in [-1, 1]^2$, forming a uniform grid. Each neuron's RF was modeled as a 2D Gaussian filter centered at (x_i, y_i) :

$$w_i(x,y) = \exp\left(-\frac{(x-x_i)^2 + (y-y_i)^2}{2\sigma^2}\right),$$
 (61)

where $\sigma = 0.1$ defines the spatial extent of the RF, and (x_i, y_i) specifies the center of the *i*-th neuron's RF. These centers were evenly spaced across the image grid.

Neural firing rates were computed by projecting the input image I onto the receptive field weights w_i , followed by a sigmoid nonlinearity:

$$f_i = A \cdot \frac{1}{1 + \exp(g \cdot w_i^\top (I + 1 - \theta))},\tag{62}$$

where A=40 is the amplitude, g=0.4 is the gain and $\theta=0.9$ is the threshold. This yields the mean firing rate of neuron i in response to image I.

To capture neural variability, we modeled spike counts as samples from a Poisson distribution with mean f_i .

C.3 Diffusion Models

We trained two denoising diffusion probabilistic models (DDPMs) based on the *UNet-2D* architecture Ronneberger et al. [2015], using the implementation provided by the HuggingFace diffusers library von Platen et al. [2022].

The first model was trained to generate MNIST digits from standard Gaussian noise $Z \sim \mathcal{N}(0, I)$. Following the DDPM framework Ho et al. [2020], we simulated a forward diffusion process that progressively adds Gaussian noise to an image x_0 , producing a sequence of noisy images $\{x_t\}$. The process is defined as:

$$x_t = \sqrt{1 - \beta_t} \cdot x_{t-1} + \sqrt{\beta_t} \cdot z_t, \quad z_t \sim \mathcal{N}(0, I), \tag{63}$$

where β_t denotes the noise schedule. By recursively applying this equation, one obtains:

$$x_t \sim \mathcal{N}\left(\sqrt{\bar{\alpha}_t} \cdot x_0, (1 - \bar{\alpha}_t)I\right), \quad \text{with} \quad \bar{\alpha}_t = \prod_{s=1}^t (1 - \beta_s).$$
 (64)

Although this differs from the isotropic Gaussian noise model used in the main text, $x_t = x_0 + \sqrt{\gamma}Z$, the two formulations are equivalent up to reparameterization, with $\gamma = \frac{1-\bar{\alpha}_t}{\bar{\alpha}_t}$. Thus, both can be used interchangeably to estimate the information decomposition $I_{\rm local}(x)$.

We used a linear noise schedule with β_t increasing from 1×10^{-4} to 0.02 over 1,000 time steps. Given a noisy image x_t , the model was trained to predict the noise component $\hat{z}_t(x_t)$, which can be used to reconstruct an estimate of the clean image:

$$\hat{x}(x_t) = \frac{x_t - \sqrt{1 - \bar{\alpha}_t} \cdot \hat{z}_t(x_t)}{\sqrt{\bar{\alpha}_t}}.$$
 (65)

A second DDPM was trained using the same architecture, but conditioned on simulated neural responses r (see previous section). This model learned to predict the noise given both the noisy image and response:

$$\hat{x}(x_t, r) = \frac{x_t - \sqrt{1 - \bar{\alpha}_t} \cdot \hat{z}_t(x_t, r)}{\sqrt{\bar{\alpha}_t}}.$$
(66)

We used these models to estimate the pixel-wise information decomposition described in the main text (Eq. 9). To approximate the integral over γ , we applied additive Gaussian noise according to the diffusion schedule and evaluated $\hat{x}(x_t)$ and $\hat{x}(x_t,r)$ over 24 diffusion steps (indexed as [40:40:1000]) using 50 noisy samples of x_t and r at each t. On average, approximating $I_{local}(x)$ for one image took approximately 1 minute on an NVIDIA GeForce RTX 4080 GPU.

C.4 Training Details

Both models were implemented in PyTorch (version 2.7.0) with Cuda 12.6 and trained using the HuggingFace Diffusers library von Platen et al. [2022] and Accelerate library Gugger et al. [2022] for distributed training on 7 NVIDIA A100 GPUs (40 GB VRAM).

The training procedure for both models was as follows:

• Optimizer: AdamW with learning rate 1×10^{-4} , $\beta_1 = 0.9$, $\beta_2 = 0.999$

• Learning rate scheduler: Cosine schedule with warmup (500 steps)

• Batch size: 256

• Training duration: 150 epochs

• Loss function: Mean squared error (MSE) between predicted and true noise

• Precision: Mixed precision training with bfloat16

• Training Time: 25/30 minutes per model

C.5 Decomposition for additional digits

We repeated the analysis described in Figure 4 originally performed for two digits on six additional digits using exactly the same linear-nonlinear Poisson (LNP) model, receptive field configuration, and information decomposition procedure. For each new digit, we computed the Fisher information and the pixel-wise information $I_{\rm local}(x)$ following identical preprocessing, stimulus presentation, and estimation steps as in the main analysis.

C.6 Decomposition for natural images

To demonstrate that our approach generalizes to more complex and biologically realistic neural encoder models as well as natural images, we trained the diffusion models on $60,000~64\times64$ natural images from Hugging Face's Tiny ImageNet dataset and trained a deep neural network model of the retina Klindt et al. [2017] to replicate the responses of 41 retinal ganglion cells (RGCs) from Goldin et al. [2022]. We extended the model by tiling the stimulus space with a 7×7 square lattice mosaic of receptive fields, where the resulting 49-field mosaic reproduced the response pattern of one of the fitted cells. As with the MNIST digits, we then applied pixel-wise information decomposition to natural images (Fig. 7). Consistent with our findings for the MNIST stimuli, the resulting local information maps, $I_{\rm local}(x)$, exhibited the highest values in regions of high spatial contrast, particularly along object boundaries, indicating that these areas contribute most strongly to the encoded information about the stimulus.

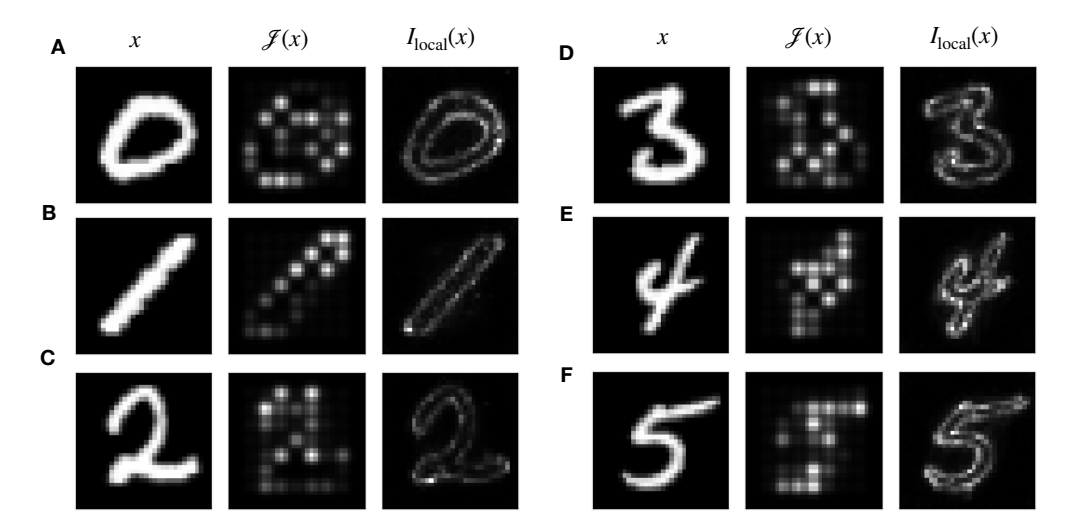


Figure 6: **Information decomposition across additional digits.** In the main text, we present pixel-wise information decomposition for two example digits. Here, we provide several additional examples to illustrate the decomposition patterns across other digits.

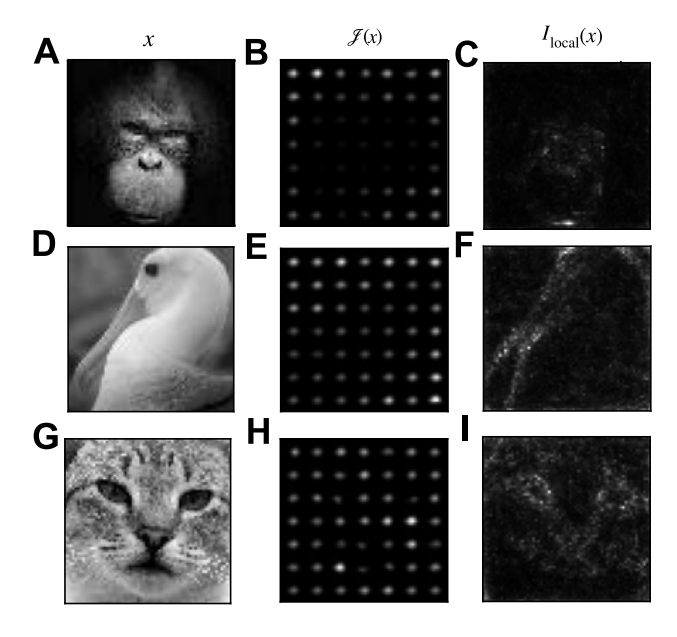


Figure 7: **Pixel-wise information decomposition with natural image stimuli.** (A) Presented visual stimulus. (B) Fisher information was computed as the sum of each neuron i's pointwise contribution, $(f_i'(x))^2/f_i(x)$, quantifying the local neural sensitivity to infinitesimal changes in the intensity of pixel x. (C) Pixel-wise decomposition of mutual information, $I_{local}(x)$. **D-I** Same as panels A-B, but for different stimuli.

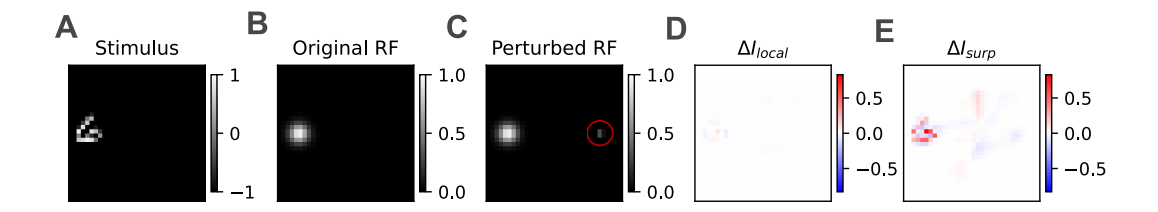


Figure 8: Illustration of the locality of $I_{\rm local}(x)$ compared to $I_{\rm surp}(x)$. (A) The visual stimulus is a MNIST digit positioned on the center-left side of the visual field. (B) Receptive field of LNP model neuron 21 in the unperturbed condition, located on the center-left side of the visual field (the remaining 48 receptive fields are unperturbed and not shown). (C) The receptive field of neuron 21 is modified by adding a sharp 2D Gaussian perturbation (highlighted by a red circle) on the opposite side of the stimulus. (D) Difference in $I_{\rm local}(x)$ and (E) difference in $I_{\rm surp}(x)$ between the original and perturbed receptive field conditions. $I_{\rm local}(x)$ remained confined near the stimulus and the perturbed receptive field, reflecting its local nature, while $I_{\rm surp}(x)$ exhibited broader, spatially distributed changes.

C.7 Demonstration of locality for MNIST stimuli

To further illustrate the locality properties of the information decomposition, we examined how a small, spatially localized perturbation to a single receptive field affects $I_{\rm local}(x)$ and $I_{\rm surp}(x)$. We used the same linear–nonlinear–Poisson (LNP) model described in the main text, with receptive fields arranged across the visual field (Supplementary Figure 8B). In the perturbed condition, we introduced a sharp two-dimensional Gaussian bump to the receptive field of a single neuron, located on the opposite side of the visual stimulus (Figure 8C).

We then computed the pixel-wise differences in $I_{\rm local}(x)$ and $I_{\rm surp}(x)$ between the perturbed and unperturbed conditions. As shown in Figure 8D–E, $I_{\rm local}(x)$ remained confined to the vicinity of the stimulus and the affected receptive field, reflecting its inherently local nature. In contrast, $I_{\rm surp}(x)$ exhibited broader, spatially distributed changes, highlighting its global dependence on the overall structure of the neural population code.

The code repository to reproduce figure 4, 6, 7 and 8 can be found at neural-info-decomp.